

4.2.3

Airfoil Endwall Heat Transfer



Karen Thole

Mechanical Eng. Dept, Penn State Univ,
University Park, PA 16802-1412

phone: (814) 865-2519
email: kthole@psu.edu

4.2.3-1 Introduction

The flow in a gas turbine influenced by the inner hub and outer casings of the airfoils is defined as secondary or endwall flows. These flows often contain vortices that give rise to velocity components that are orthogonal to the primary flow direction as depicted in figure 1 by the ribbon arrows, which is specific to vane endwalls. These flows constitute one of the most commonplace and widespread three-dimensional flows arising in axial flow turbomachinery. In typical modern day turbine designs, endwall flows for first stage vanes are responsible for over 30% of the total pressure loss through a turbine stage leading to a reduction in turbine efficiencies on the order of 3%. While overall airfoil losses have been reduced through the use of three-dimensional geometries that make use of bowed or leaned airfoils, for example, the endwalls have remained fairly conventional and the source of much of the remaining pressure losses. The heat transfer consequences are immense because of the increased convective coefficients and mixing out of film-coolant near the surface. It is clear from a thermodynamic analysis of a turbine engine, that to improve performance, there is a need to increase the aspect ratio for turbine airfoils and to increase turbine inlet temperatures. To improve a turbine's performance, these trends require that endwall flows be carefully considered in turbine designs.

The endwall flow through an airfoil cascade under isothermal conditions with an approaching two-dimensional boundary layer agrees well with that depicted in figure 1. The flow model shows that the inlet boundary layer separates from the approaching endwall to form what is known as a horseshoe vortex. One leg of the horseshoe vortex, present on the pressure side of the airfoil (concave side), is convected into the passage and is promoted by the inherent pressure gradient between the two airfoil surfaces. This pressure side leg of the horseshoe vortex develops into what is known as the passage vortex. The other leg of the horseshoe vortex, present on the suction side of the airfoil (convex side), has an opposite sense of rotation to the larger passage vortex and develops into what is known as a counter vortex. The counter vortex can be thought of as a planet rotating about the axis of the passage vortex (sun). The actual rotation of the vortices depicted in figure 1 were drawn to exaggerate the vortex motion and for the passage vortex is generally about two rotations before exiting the airfoil passage. While this picture represents a time-averaged representation, measured data indicates that the vortex is not steady. While the development of the vortical structures originates in the endwall regions, the growth can be such that the passage vortex occupies a large portion of the airfoil exit. This

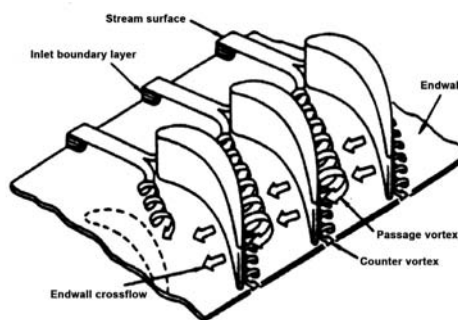


Fig. 1. Classic secondary flow pattern for a turbine airfoil passage. (reproduced with permission from American Society of Mechanical Engineers [ASME]).

Source: Langston, L. S. "Crossflows in a Turbine Cascade Passage," *ASME J of Engineering for Power* 102 (1980): 866 - 874.

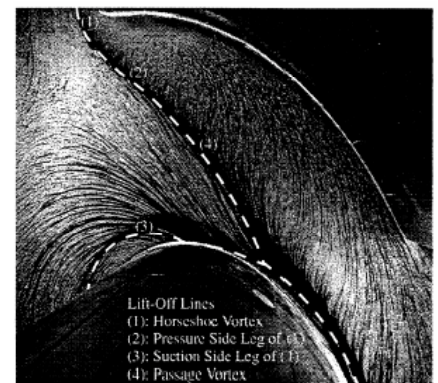


Fig. 2. Illustration of the near wall flows as taken through oil and dye surface flow visualization (reproduced with permission of the publisher from ASME).

Source: Friedrichs, S., Hodson, H. P. and Dawes, W. N., "Distribution of Film-Cooling Effectiveness on a Turbine Endwall Measured Using the Ammonia and Diazo Technique," *J of Turbomachinery* 118 (1996): 613-621.

vortical structure growth extends up to 30-40% of the total span for older vane designs and has been reduced to approximately 10-15% of the total span in the last 15 years.

The flow patterns previously described make it difficult to cool the endwall, particularly when considering the near endwall flow, as illustrated in figure 2. The surface flow visualization in figure 2, achieved through an oil and surface dye technique, illustrates the strong cross flows that occur. The cross flows are driven by the inherent pressure gradients from the pressure to the suction side of adjacent airfoils. For example, these cross flows influence how the film-cooling jets exit from the holes as well as influence the endwall heat transfer coefficients.

This section briefly describes a simplified theoretical approach to understanding vane endwall flows. Following this brief discussion the following will be provided: heat transfer coefficients experienced along a turbine vane endwall with varying effects, film-cooling designs, and geometrical means for reducing endwall heat transfer. Outer casing flows of vanes are similar to inner hub flows; however, for blades the outer casing flows encompass yet another difficult region which is the blade tip region. Generally, there is a gap between the blade tip and outer casing that provides for a leakage flow that is inherently driven by the pressure difference between the pressure and suction sides of the blades. A brief section about tip flows will be provided at the end of this section.

4.2.3-2 Theoretical Development of Endwall Flows

As the endwall boundary layer approaches a turbine airfoil, the flow stagnates, whereby the total pressure becomes the static pressure along the span of the vane. Given that the fluid nearer to the endwall has a lower velocity, a stronger deceleration in the boundary layer occurs for the higher speed fluid than for the lower speed fluid. As a result of these differences in the deceleration, a transverse static pressure gradient occurs along the vane span causing the higher speed fluid to turn toward the endwall plate. Subsequently, the formation of a horseshoe vortex occurs just upstream of the turbine vane. One of the legs of the horseshoe vortex wraps around the pressure side of the vane and the other leg wraps around the suction side of the vane. Figure 3a shows measurements of the horseshoe vortex upstream of the turbine vane and figure 3b shows extreme damage from the effects of this vortex on actual hardware. These measurements were made for a simple case with an isothermal flow and an approaching boundary layer that was 9 % of the vane span ($Z/S = 0.09$). From the combined contour/vector plot in figure 3a, one can see where the flow separates from the upstream endwall and how the flow is then rolled into a vortex. It is also clear to see that, if a film-cooling jet were injected into this region, it would be difficult to maintain the coolant along the endwall.

The flow fields discussed thus far have described the condition for a uniform, isothermal flow field with an approaching two-dimensional boundary layer along the endwall. In practice, this idealized flow situation rarely happens since an upstream combustor is present whereby there can be large variations in the exiting flow. Non-uniformity of inlet profiles in addition to the viscous boundary layers along the endwall are caused by temperature gradients at the combustor exit. The development of cross-flow and vortical motions in a curved passage, such as an airfoil passage, can be understood by considering flow along two streamlines, as shown in figure 4. Two idealized cases are considered: a) a gradient of velocity due to a turbulent inlet boundary layer with an isothermal flow, b) a linear temperature gradient typical at the exit of a combustor with a uniform velocity field.

Assuming steady, incompressible, inviscid flow with negligible variation of velocity in the n -direction, the centripetal acceleration for the streamlines A and B must be balanced by the pressure gradient across the pitch:

$$\left. \frac{\partial p}{\partial n} \right|_A = \rho \frac{V_{S A}^2}{R_A} \quad \left. \frac{\partial p}{\partial n} \right|_B = \rho \frac{V_{S B}^2}{R_B} \quad (1)$$

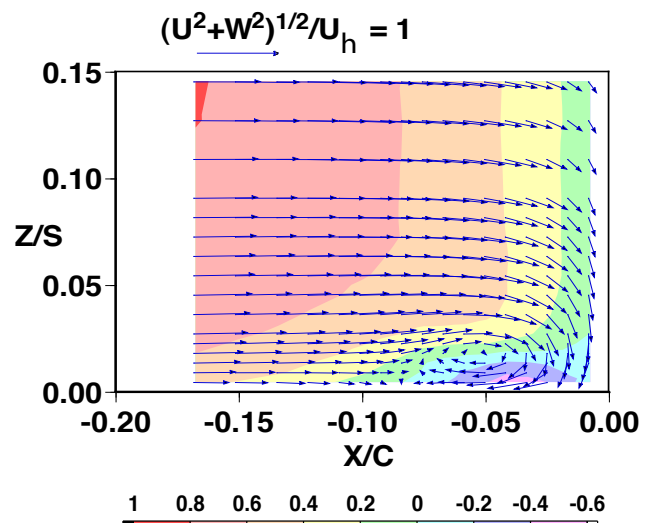


Fig. 3a. Measurements of the horseshoe vortex just upstream of the vane at the vane-endwall juncture (reproduced with permission from ASME).

Source: M. Kang, A. Kohli, and K.A. Thole, "Heat Transfer and Flowfield Measurements in the Leading Edge Region of a Stator Vane Endwall," *J of Turbomachinery* 121 (1999): 558-568.



Fig. 3b. Actual hardware showing effects of the horseshoe vortex on a first vane

From boundary layer theory, $\frac{\partial p}{\partial n}$ for both streamlines from the developing boundary layer on the sidewalls should be equal. Therefore

$$\left. \frac{\partial p}{\partial n} \right|_A = \left. \frac{\partial p}{\partial n} \right|_B \quad (2)$$

Due to the viscous turbulent boundary layer at the endwall, it is evident that $V_{sB} < V_{sA}$. So for the boundary layer assumption to hold, the radius of curvature of the streamline at B must be reduced. This creates a crossflow in the boundary layer from the pressure surface towards the suction surface of the blade, and thus generates secondary flow (flow that is not aligned with the streamwise direction) as depicted in figure 4a.

Now consider figure 4b, a constant velocity profile with linear temperature profile. The same physics hold for this case; however, the resulting vortex is reversed in direction. In this instance the temperature at A is greater than at B, therefore $\rho_A < \rho_B$. Now R_B must be greater than R_A for the normal pressure gradient to balance and the cross flow is generated towards the pressure side of the adjacent vane row. The change in streamline curvature would be less severe in this case compared to figure 4a since the velocity term is squared in the relationship of Equation 1.

As one can see from these simple, idealized flow situations, there can be large variation in the expected secondary flow pattern that can be derived in a turbine vane passage. The important driver for how the flow develops in a turbine vane passage is the total pressure profile entering the passage. As this total pressure profile becomes the static pressure along the vane stagnation, the flow will be driven from a high pressure region to a low pressure region. In most turbine designs there is a flow leakage slot between the combustor and the turbine whereby cooler fluid is injected into the main hot gas path. This leakage can also have an effect on the secondary flow patterns that develop. The bottom line when considering endwall flows is that the profile exiting the combustor, which is often referred to as the combustor pattern factor that ultimately enters the turbine, should be known to fully predict the secondary flows that will develop in the turbine passage. In practice, the combustor pattern factor is one of the parameters used in designing cooling schemes for the airfoils and their associated platforms.

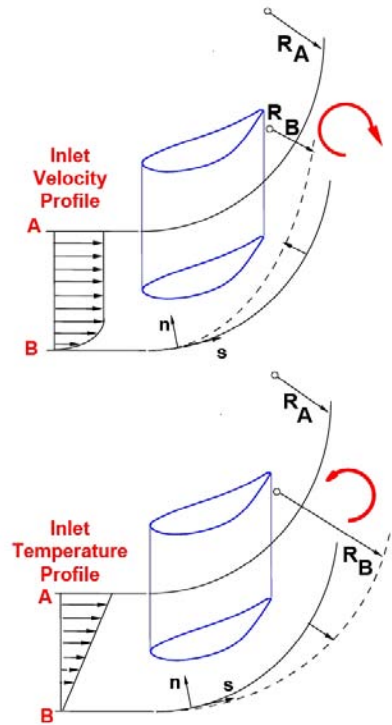


Fig. 4. Illustration of different vortical patterns that are possible for two idealized flow conditions: a) isothermal with an inlet boundary layer and b) inviscid flow with a temperature profile.

Source: B. Lakshminarayana, Fluid Dynamics and Heat Transfer of Turbomachinery (NY: Wiley Interscience, 1996).

4.2.3-3 Endwall Heat Transfer

The heat transfer coefficients given in figure 5 are represented in terms of a non-dimensional Stanton number based on exit velocity. In the region upstream of the vanes, there is a high heat transfer region that occurs between the stagnation point and the reattachment of the flow on the suction side of the airfoil. This is the area which experiences very high acceleration. As the flow moves through the passage, it is apparent that the location of the peak Stanton numbers (peak heat transfer) is being swept from the outer pressure surface towards the suction side of the central vane.

Figure 6 presents the Stanton numbers for two freestream turbulence levels ($Tu = 0.6\%$ and 19.5%) approaching the stagnation location along a line parallel to the incoming velocity vector. Figure 6 illustrates that at a location of approximately 15% of the chord ($\Delta X/C = 0.15$) upstream of the vane, the Stanton numbers begin to increase dramatically. This increase can be related to the position where the flow separates from the endwall, as shown by Figure 3a, which occurs at approximately $X/C = 0.12$. The heat transfer continues to increase as the flow approaches the vane.

Depending upon the particular combustor design, the turbulence levels exiting a combustor that enter into the turbine can be relatively high. In general, high levels of turbulence lead to higher levels of heat transfer. Figure 6 illustrates this increase through both the Stanton numbers (left axis) and the augmentation of Stanton numbers (right axis) whereby augmentation refers to the Stanton number (convective heat transfer coefficients) at high turbulence divided by the Stanton number at low turbulence levels. Figure 6 illustrates that there is an approximate 20% increase in heat transfer resulting from a turbulence level of 19.5%.

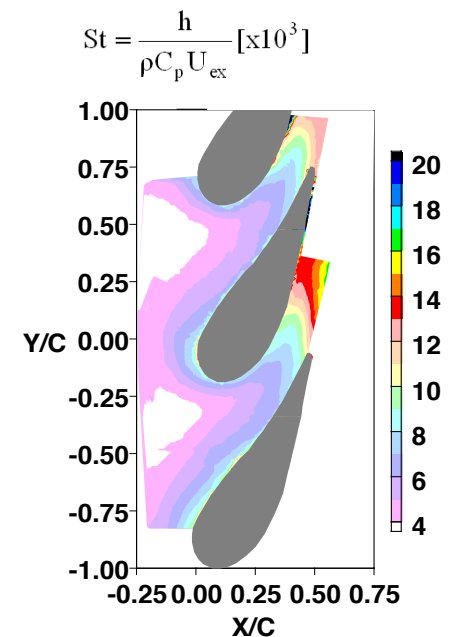


Fig. 5. Contours of non-dimensional heat transfer coefficients (reproduced with permission from the publisher of ASME).

Source: See fig. 3a above.

4.2.3 Airfoil Endwall Heat Transfer

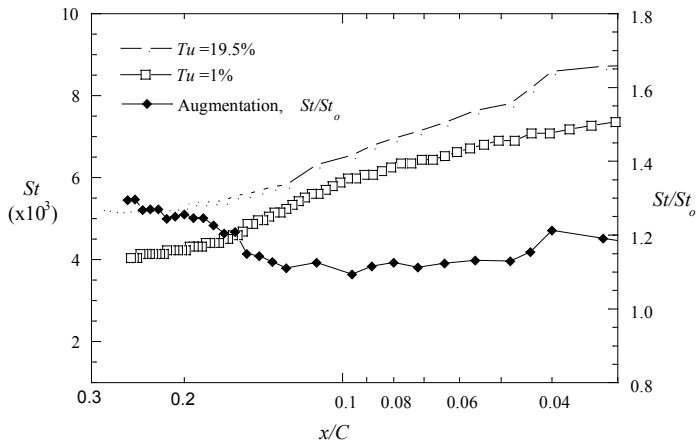


Fig. 6. Non-dimensional heat transfer coefficients (left axis) along the endwall approaching the vane leading edge for low (St_0) and high freestream turbulence (St); and augmentation factors (right axis) for heat transfer coefficients (reproduced with permission from the publisher of ASME).

Source: R. Radomsky and K. Thole, "High Freestream Turbulence Effects in the Endwall Leading Edge Region," *ASME J. of Turbomachinery* 122 (2000): 699-708.

Figure 7 compares the heat transfer coefficients averaged over the pitch (vane-to-vane) for a range of axial positions. As the flow accelerates through the passage, the heat transfer coefficients also increase, which is to be expected. For most of the axial distance, the augmentation due to freestream turbulence is relatively constant at 25% above the low freestream turbulence case. Only near the end of the vane where the passage vortex dominates, beyond X/C of 0.38, is there a decrease in the augmentation.

Note that the heat transfer data shown in this paper were taken with a two-dimensional inlet boundary layer under low speed conditions, to allow for highly-resolved data, with matched Reynolds number conditions. There is evidence in the literature that the secondary flow patterns remain the same at both low and high Mach number conditions. Rather, these secondary flows are a stronger function of the airfoil geometry and inlet profile conditions than of Mach number. There is no data in the literature that discusses how the heat transfer on the endwall is altered depending upon an inlet flow condition that is relevant to that exiting a combustor. As was stated previously, it is important to consider that the profile exiting the combustor can vary greatly from that of a two-dimensional boundary layer assumption.

4.2.3-4 Endwall Film-Cooling

One method of combating the high heat transfer coefficients along the endwall is through the use of film-cooling holes whereby cooler air is injected through discrete holes in the endwall. Film-cooling hole placement, particularly in the endwall region, has traditionally been based upon designer experience whereby a number of design variables are considered. For example, one should take into account leakage from a slot at the combustor-turbine interface whereby cooler gases leak into the main gas path (combustor film-cooling carryover). Most turbines are designed such that pressures outside the main gas path are higher than those found in the main gas path to insure that the hot combustion gases are not ingested below the platform. If designed properly, this leakage flow could be relied upon as a source of coolant. It is also important to remember that the secondary flows that develop are affected by the leakage flows at the vane inlet, as indicated by the previous discussion in this section. Other design variables include roughness effects, film-cooling migration (as will be discussed), film-cooling limitations resulting from internal cooling schemes, and cooling hole manufacturing. Manufacturing of cooling is generally done through the use of electro-discharge machining (EDM) or laser drilling with both being subjected to access limitations. Generally, EDM is more expensive than laser drilling and conversely laser drilling can tend to be more limited in terms of hole geometries that can be manufactured.

Consider a leakage slot flow between the combustor and turbine whereby the coolant is 0.75% of the core flow. The cooling to the endwall that can be provided is shown in figure 8. Coolant exits across much of the width of the slot albeit in a very non-uniform manner. This non-uniform slot flow arises from the static pressure distribution and secondary flow development along the endwall. Although there is a large uncooled region,

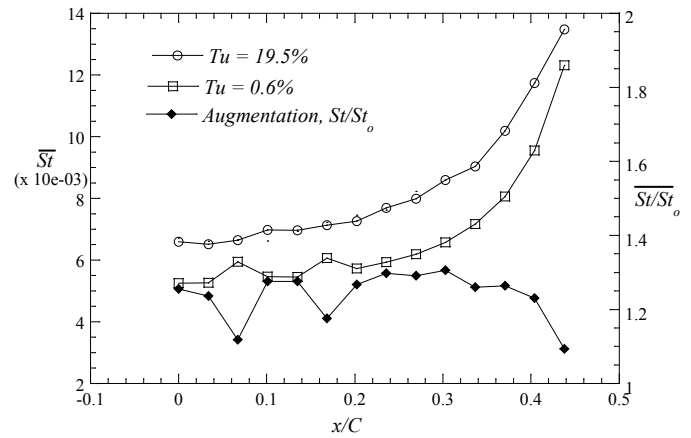


Fig. 7. Pitchwise averaged non-dimensional heat transfer coefficients (left axis) for low and high freestream turbulence; and augmentation factors (right axis) for heat transfer coefficients (reproduced with permission from the publisher of ASME).

Source: See fig. 6 above.

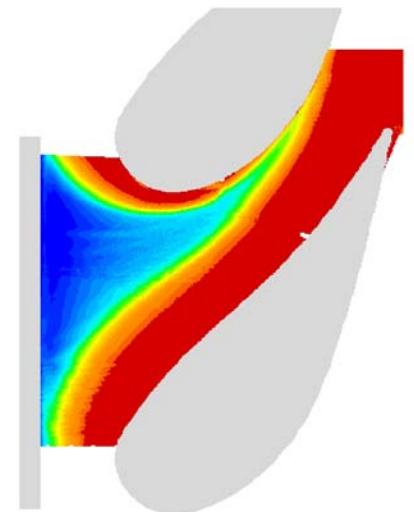


Fig 8. Measured adiabatic wall temperatures for coolant exiting a combustor/vane leakage slot (reproduced with permission from the publisher of ASME).

Source: D.G. Knost and K. Thole, "Adiabatic Effectiveness Measurements of Endwall Film-Cooling for a First Stage Vane," *J. of Turbomachinery* 127 (2005): 297-305.

often referred to as a bow wake, around much of the vane at the leading edge and along the pressure side of the airfoil, there is also a well-cooled region in the center of the passage. As the slot flow increases, the cooling potential also increases to a point after which the benefit is small.

As was previously mentioned, endwall film-cooling has largely been based on designer experience. One difficulty in designing the film-cooling hole pattern is knowing beforehand the local static pressure along the endwall, which varies greatly along the endwall as the flow accelerates through the passage. If one considers that a single supply feeds all the film-cooling holes and inviscid flow through the holes, it can be shown that a global, ideal (loss-free) blowing ratio for all the film-cooling holes is given by the following equation,

$$M_{\text{global}} = \frac{\rho_c U_c}{\rho_{\text{in}} U_{\text{in}}} \sqrt{\frac{\rho_c}{\rho_{\text{in}}} \cdot \frac{P_{o,c} - p_{s,\text{in}}}{P_{o,\text{in}} - p_{s,\text{in}}}} \quad (3)$$

where $P_{o,\text{in}}$ and $p_{s,\text{in}}$ are defined at the inlet to the turbine. If one then wants to compute the local, ideal blowing ratio for each cooling hole (now taking into consideration that the local velocity varies), the following equation can be used

$$M = \frac{\rho_c U_c}{\rho_{\infty} U_{\infty}} = \sqrt{\frac{\rho_c}{\rho_{\text{in}}} \cdot \frac{P_{o,c} - p_{s,\infty}}{P_{o,\text{in}} - p_{s,\infty}}} \quad (4)$$

where $p_{s,\infty}$ is the local static pressure defined at the exit of the cooling hole. Equation 4 indicates that the same blowing ratio will occur for each hole placed along a constant static pressure line. Designing an endwall cooling pattern to achieve a uniform blowing ratio is one methodology that some companies have used.

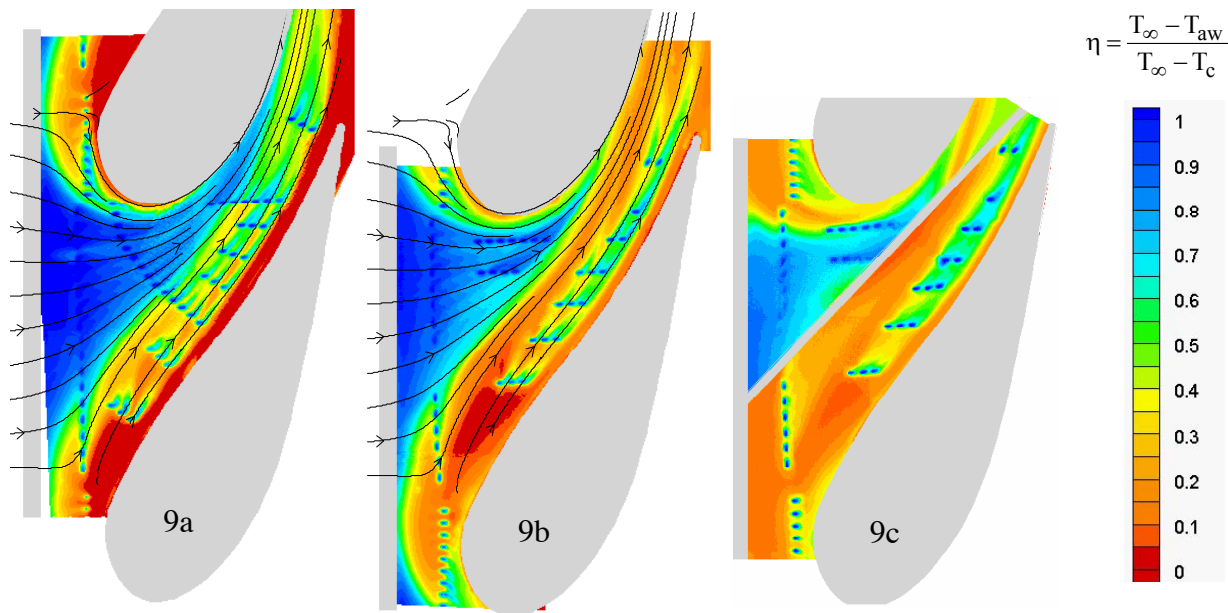


Fig. 9. Contours of adiabatic effectiveness for two film-cooling hole patterns (left and center) with a mid-passage gutter for the cooling hole pattern in the center (right) (reproduced with permission from the publisher of ASME).

Source: See figure 8 above.

Figure 9a shows a cooling hole pattern whereby the holes in the passage were placed along a constant static pressure line. Figure 9b shows an endwall cooling hole pattern with holes that were placed on lines parallel to the incoming flow direction. The endwall in Figure 9b also provides the space for including a mid-passage gap that occurs between vanes as the vanes are mated on the turbine disk. Vanes are generally cast in either doublets or singlets and then placed in a turbine disk with some type of seal between the vane platforms. Generally, relatively low levels of coolant leak from this mid-passage gap (less than 0.3%). Figure 9c shows the same film-cooling hole pattern as that in figure 9b with the exception being the mid-passage gap is present in figure 9c.

The coolant flow conditions for all three vanes shown in figure 9 are the same with 0.75% of the core flow exiting in the form of coolant from the upstream slot, 0.5% coolant exiting the film-cooling holes and no net coolant flow through the mid-passage gap for figure 9c. The contours plotted in figure 9 represent the non-dimensional adiabatic wall temperatures. As discussed in the previous section, adiabatic surface temperatures represent the local fluid temperature. From all three contour plots in figure 9, it is clear that the upstream slot can definitely be an important part of cooling mid portion of the endwall. In comparing figure 9c to the rest, however, it

4.2.3 Airfoil Endwall Heat Transfer

is also seen that the mid-passage gap limits the area of the cooling present. The mid-passage gap provides a convective coolant trough through which coolant from the upstream slot enters and passes through the gap along the mid-passage before exiting the gap near the trailing edge of the airfoil.

The streamlines superimposed upon the experimental measurements of the adiabatic wall temperatures presented in figure 9, were computed using computational fluid dynamics (CFD). These streamlines were extracted from the CFD simulations at a location very near to the endwall (less than 2% of the span). The streamlines, for the most part, can be used to predict the trajectory of the coolant flow exiting the cooling holes. There are some regions, however, where the streamlines differ from the jet trajectories, such as at the entrance to the passage closer to the pressure side.

In comparing all of the cooling hole patterns in figure 9, it is clear that more uniform cooling can be achieved by placing cooling holes along constant static pressure lines as in figure 9a. All three patterns illustrate the difficulty of cooling the endwall along the pressure side of the vane and along the leading edge-endwall juncture. In general these are very difficult areas to cool because of the secondary flows that were described previously. The horseshoe vortex in the stagnation region can lead to coolant being swept upstream of the holes at low blowing ratios, whereas at high blowing ratios the coolant separates from the endwall and impacts the vane surface rather than the endwall surface. Despite the cooling holes injecting coolant towards pressure side of the vane, the sweeping motion of the passage vortex prevents cooling at the juncture between the pressure side of the vane and the endwall.

4.2.3-5 Leading Edge Modifications

Because industry is concerned with problems at the vane leading edge-endwall juncture, a number of more recent studies have begun to evaluate geometric modifications to airfoils in this region. Both overall vane endwall contouring, as shown in figure 10, as well as more specific geometric features particular to the leading edge region have been considered. At this point there have been three different geometric concepts tested for an asymmetric airfoil geometry that include the following classifications: fences, fillets, and bulbs. Methods using flow control such as suction combined with injection have also been reported but are generally not feasible for gas turbines where gas temperatures exceed airfoil melting temperatures. Chung and Simon first presented their concept for secondary flow control in 1993 that encompassed using a fence placed in mid-passage between two turbine airfoils¹. While their tests indicated a reduction in strength of the passage vortex, industry's concern was in cooling the fence and that it acted as a fin conducting heat to the platform as it was exposed to the hotter main gas path fluid.

While the fillet and bulb appear to be similar, as shown in figure 11a, the physical concepts behind why there are these two different modifications are quite different. Sauer et al. and Becz et al. studied the effects of various sized leading edge endwall bulbs as shown in figure 11a.² The objective of this modification was to intensify the suction side branch of the horseshoe vortex and, through an interaction of the stronger suction side branch with the passage vortex, weaken the passage vortex. Becz et al. found that when compared with a fillet geometry, such as that shown in figure 11b, there were slightly lower aerodynamic losses for a fillet rather than a bulb³.

The philosophy behind the Zess and Thole modification, which was a fillet as shown in figure 11b, was to eliminate the leading edge vortex thereby delaying the development of the passage vortex⁴. They presented a direct comparison between measured and predicted flow fields for an airfoil with no fillet and an airfoil with a fillet design. Their results indicated no presence of a leading edge vortex for a filleted airfoil and a delayed passage vortex. Moreover, their experimental results indicated a large reduction (by more than an order of magnitude in some locations) of turbulence levels for a filleted airfoil.

The only papers to have considered the endwall heat transfer effects has been that of Shih and Lin, Lethander and Thole, and Han and Goldstein (who both performed computational studies to evaluate different fillet designs)⁵. Shih

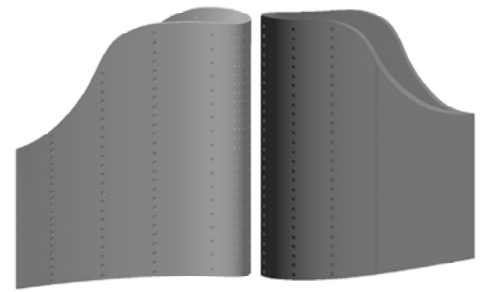


Fig.10. Example of contoured endwall for a first vane design

Source: W. Colban, K. Thole, and M. Haendler, "Heat Transfer and Film-Cooling Measurements on a Stator Vane with Fan-Shaped Cooling Holes," International Gas Turbine and Aeroengine Congress and Exposition, Reno, GT2005-68258.

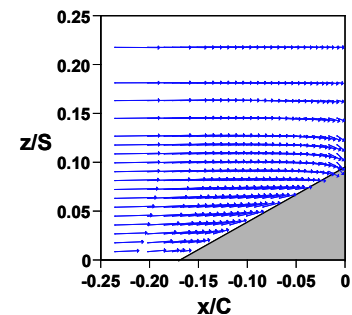
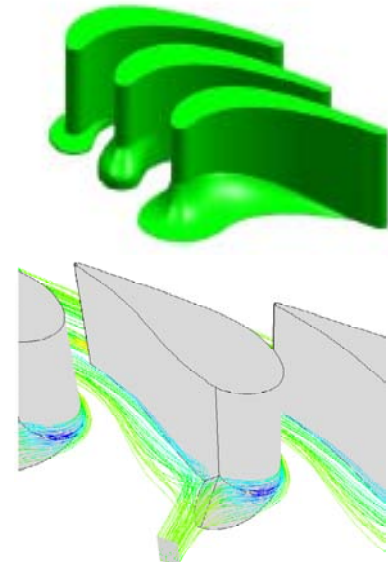


Fig.11. Various leading edge geometries: a) fillet and bulb designs as shown by Becz et al. and b) CFD predictions and flowfield measurements for a filleted vane by Zess and Thole (reproduced with permission from the publisher of ASME).

Sources: See notes 2 and 4.

and Lin, investigated not only the use of a leading edge modification but also of inlet swirl to control secondary flows in an airfoil passage. Two different modifications along with no modification were considered for three different inlet swirl configurations: no swirl and swirls of opposite rotation with linearly varying swirl angle from endwall to endwall. The two modifications differed in how they blended into the vane geometry with one fading into the vane surface and the other fading into the endwall. While no single case provided maximum reduction for every metric, a case with inlet swirl and no fillet came very close to doing so. In comparison, the aerodynamic and heat transfer benefits realized for cases with fillets and no inlet swirl were not as great. The computational work by Lethander and Thole combined a three-dimensional computational fluid dynamics (CFD) package along with an optimization package to design an optimal fillet with a rather limited number of independent parameters. Given their specified constraints, the results from their optimization study indicated a successful fillet design was one that was relatively large. While their aerodynamic losses were predicted to slightly increase with their optimal fillet, the thermal environment for the airfoil platform was significantly reduced. Han and Goldstein used the fillet design of Zess and Thole and found that there was a reduction in heat transfer but only near the leading edge-endwall juncture⁶. In the downstream portion of the passage there was little reduction.

Three-dimensional endwall contouring, which includes a more comprehensive geometric modification than simply a modification to the endwall-airfoil leading edge juncture, has also been investigated computationally by Harvey, et al. and experimentally verified by Hartland, et al.⁷. To design the endwall contour, they used a linear sensitivity matrix in conjunction with superposition methods prior to applying an inverse design algorithm. The results of the experimental verification confirmed a predicted reduction in exit flow angle deviations. Moreover, the experiments indicated a 30% reduction in loss, which was higher than predicted. In a later study, Brennan, et al. and Rose, et al. applied similar computational and experimental (respectively) methodologies as Harvey et al. and Hartland, et al.⁸. They applied these methods to a high pressure turbine for a single stage in both the vane and blade passages. They reported stage efficiency improvements of 0.59%, which exceeded their predicted improvement of 0.4%.

Using endwall contouring and leading edge modifications show promise in reducing secondary flows; however, there are numerous effects that need to be considered. Because this modification must be practically feasible, required manufacturing, space limitations, and cooling are all practical issues that must be addressed. Moreover, some of these designs may be sensitive to the inlet flow conditions which need to be considered.

4.2.3-6 Other Relevant Vane Endwall Studies

As discussed in the previous section, a number of studies have been completed with regards to vane endwalls. To form a more complete list of studies presented in the literature on this topic, this section describes additional studies of interest.

Blair measured adiabatic effectiveness levels and heat transfer coefficients for a range of blowing ratios through a flush slot placed just upstream of the leading edges of a single passage channel⁹. One of the key findings was that the endwall adiabatic effectiveness distributions showed extreme variations across the vane gap with much of the coolant being swept across the endwall toward the suction side corner. Granser and Schulenberg reported similar adiabatic effectiveness results in that higher values occurred near the suction side of the vane¹⁰.

One of the more detailed endwall film cooling studies have been conducted by Friedrichs et al.¹¹. The results of their studies indicated that the endwall cross-flow was altered so that the cross-flow was turned toward the inviscid streamlines as a result of film-cooling injection. There have been a few studies that have measured endwall heat transfer as a result of injection from a two-dimensional, flush slot just upstream of the vane.

A series of experiments have been reported for various injection schemes upstream of a nozzle guide vane with a contoured endwall by Burd and Simon, Burd et al., and Oke et al.¹². In the studies presented by Burd and Simon, Burd et al. and Oke et al., coolant was injected from an interrupted, flush slot that was inclined at 45° just upstream of their vane¹³. Similar to others, they found that most of the slot coolant was directed toward the suction side at low slot flow conditions. As they increased the percentage of slot flow to 3.2% of the exit flow, their measurements indicated better coverage occurred between the airfoils.

Colban et al. reported flow field and endwall effectiveness contours for a backward-facing slot with several different coolant exit conditions¹⁴. Their results indicated the presence of a tertiary vortex that developed in the vane passage due to a peaked total pressure profile in the near-wall region. For all of the conditions simulated, the effectiveness contours indicated the coolant from the slot was swept towards the suction surface. While this study was completed for the same vane geometry as that reported in our paper, the slot geometry had been altered to be flush with the endwall surface.

In addition to the previously mentioned studies, the only other studies to have combined an upstream slot with film-cooling holes in the passage of the vane were those of Kost and Nicklas and Nicklas¹⁵. One of the most interesting results from the Kost and Nicklas, and Nicklas studies was that they found for the upstream leakage slot flow alone, which was 1.3% of the passage mass flow, the horseshoe vortex became more intense. This increase in intensity resulted in the slot coolant being moved off of the endwall surface and heat transfer coefficients that were over three times that measured for no slot flow injection. They attributed the strengthening of the horseshoe vortex to the fact that for the no slot injection the boundary layer was already separated with fluid being turned away from the endwall at the injection location. Given that the slot had a normal component of velocity, injection at this location promoted the separation and enhanced the vortex. Their adiabatic effectiveness measurements indicated higher values near the suction side of the vane due to the slot coolant migration.

CFD studies have also been presented to characterize the endwall film-cooling. Results presented by Knost and Thole indicated, similar to the experiments, the presence of a warm ring on the endwall (bow wave) around the vane where no coolant was present despite the combined slot cooling and film-cooling¹⁶.

4.2.3-7 Blade Tip Heat Transfer

The performance of a turbine engine is a strong function of the maximum gas temperature at the rotor inlet. Turbine blade designers concentrate on finding adequate cooling schemes for high pressure turbine blades, particularly the tip region where heat transfer is quite high. The clearance between a blade tip and its associated outer casing, also known as the blade outer air seal, provides a flow path across the tip that leads to aerodynamic losses and high heat transfer rates along the blade tip. The flow within this clearance gap is driven by a pressure differential between the pressure and suction side of the blade, and is also affected by the viscous forces as the fluid comes into contact with the walls of the gap. A complete description of blade tips and the associated problems is given by Bunker and is well described by figure 12¹⁷. Gap size, rotational effects, blade geometries and Reynolds numbers were all highly influence the heat transfer coefficients.

One method for improving the thermal environment along the blade tip is to inject coolant into the tip region. In a review paper on tip heat transfer, Bunker states that for blade tips there have been very few film-cooling studies reported in the literature even though film-cooling is widely used¹⁸. The discussion given in this section is relevant to tip film-cooling since that is what is typically used in industry.

Many tip heat transfer and film-cooling studies have been completed without rotational effects. In general, there is evidence in the literature that supports a widely variable effect of rotation, which warrants further studies. One of the first pioneers in this region is D. Metzger whereby Kim et al. presents a summary of his work¹⁹. In addition to concluding that there is only a weak effect of the relative motion between a simulated blade and shroud on tip heat transfer coefficient, they stated that there is a strong dependency of cooling effectiveness for a tip on the shape of the hole and injection locations. Four hole configurations were discussed by Kim et al. that included the following: discrete slots located along the blade tip, round holes located along the blade tip, angled slots positioned along the pressure side and round holes located within the cavity of a squealer tip. The studies reported by Kim et al. were performed in a channel that simulated a tip gap, whereby no blade with its associated flow field was simulated. In comparing the discrete slots to the holes, their data indicated a substantial increase in cooling effectiveness using the discrete slots for all blowing ratios tested. Injection from the pressure side holes provided cooling levels of similar magnitude to the holes placed on the tip with better spreading occurring in the case of the pressure side injection. Kim et al. also reported that an increase in coolant mass flow generally yielded improved cooling with tip surface holes, but for pressure side holes, increased coolant flow yielded decreased cooling effectiveness.

Kwak and Han reported measurements for varying tip gaps with cooling holes placed along the pressure surface at a 30° breakout angle and on the tip surface at a 90° angle for both flat and squealer tip geometries²⁰. They found a substantial improvement in effectiveness with the addition of a squealer tip. The coolant circulated within the squealer tip providing a better distribution of the coolant along much of the tip compared with no squealer cases. Only along parts of the suction side was the cooling effectiveness poor. They found that for the flat tip, good cooling was provided to the trailing edge due to the accumulation of coolant that exited in this area. Their results also indicated that more coolant resulted in improved effectiveness.

Results by Christophel et al. compared adiabatic effectiveness levels measured along a blade tip with injection along the pressure side of the blade²¹. Their results indicated better cooling can be achieved for a small tip gap compared with a large tip gap with different flow phenomena occurring for each tip gap setting. They also found that increased blowing leads to increased augmentations in tip convective heat transfer coefficients, particularly at the entrance region to the gap. When combined with adiabatic effectiveness measurements it was found that the coolant provided an overall net heat flux reduction to the blade tip when using film-cooling and was nearly independent of coolant flow levels.

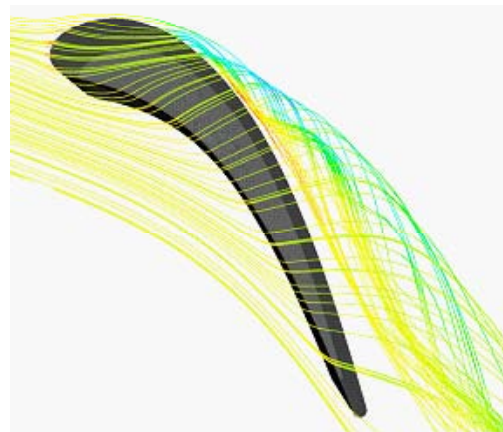


Fig. 12. CFD prediction of streamlines across a blade tip (reproduced with permission from the publisher of ASME).

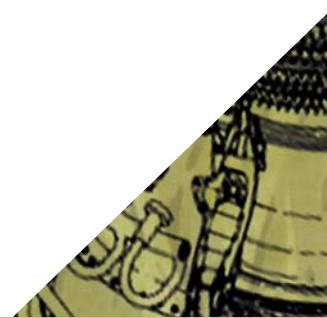
Source: E.M. Hohlfeld, J.R. Christophel, E. L. Couch, and K.A. Thole, "Predictions of Cooling from Dirt Purge Holes Along the Tip of a Turbine Blade," GT2003-38251.

4.2.3-8 Notes

1. J. T. Chung and T. W. Simon, "Effectiveness of the Gas Turbine Endwall Fences in Secondary Flow Control at Elevated Freestream Turbulence Levels," ASME 93-GT-51(1993).
2. H. Sauer, R. Müller, and K. Vogeler, "Reduction of Secondary Flow Losses in Turbine Cascades by Leading Edge Modifications at the Endwall," ASME 2000-GT-0473 (2000); S. Becz, M. S. Majewski, and L. S. Langston, "Leading Edge Modifications Effects on Turbine Cascade Endwall Loss," GT2003-38898 (2003).
3. See note 2 above.
4. G. A. Zess and K. A. Thole, "Computational Design and Experimental Evaluation of Using a Leading Edge Fillet on a Gas Turbine Vane," *J of Turbomachinery* 124 (2002): 167-175.
5. Shih, T. I-P. and Lin, Y.-L., 2002, "Controlling Secondary-Flow Structure by Leading-Edge Airfoil Fillet and Inlet Swirl to Reduce Aerodynamic Loss and Surface Heat Transfer," ASME GT-2002-30529; Lethander, A. and Thole, K. A., 2003, "Optimizing the Vane-Endwall Junction to Reduce Adiabatic Wall Temperatures in a Turbine Vane Passage," ASME Paper GT-2003-38940; Han, S. and Goldstein, R., 2005, "Influence of Blade Leading Edge Geometry on Turbine Endwall Heat (Mass) Transfer," GT2005-68590.
6. See notes 4 and 5 above.
7. J. C. Hartland, P. G. Gregory-Smith, N. W. Harvey, and M. G. Rose, "Nonaxisymmetric Turbine End Wall Design: Part II – Experimental Validation," *J of Turbomachinery* 122 (2000): 286-293; Neil W. Harvey, Martin G. Rose, Mark D. Taylor, Jonathan Shahrokh and David G. Groegory-Smith, "Nonaxisymmetric Turbine End Wall Design: Part I – Three-Dimensional Linear Design System," *J of Turbomachinery* 122 (2000): 278-285.
8. G. Brennan, N. W. Harvey, M. G. Rose, N. Fomison, and M. Taylor, "Improving the Efficiency of the Trent 500 HP Turbine Using Non-Axisymmetric End Walls: Part 1: Turbine Design," ASME 2001-GT-0444 (2001); M. G. Rose, N. W. Harvey, P. Seaman, D. A. Newman, and D. McManus, "Improving the Efficiency of the TRENT 500 HP Turbine Using Non-Axisymmetric End Walls: Part 2: Experimental Validation," ASME 2001-GT-0505(2001); also see note 7 above.
9. M. F. Blair, "An Experimental Study of Heat Transfer and Film Cooling on Large-Scale Turbine Endwalls," *J of Heat Transfer* (November 1974): 524-529.
10. D. Granser and T. Schulenberg, "Prediction and Measurement of Film Cooling Effectiveness for a First-Stage Turbine Vane Shroud," ASME Paper Number 90-GT-95 (1990).
11. S. Friedrichs, H. P. Hodson, and W. N. Dawes, "Aerodynamic Aspects of Endwall Film-Cooling," *J of Turbomachinery* 119 (1997): 786-793; S. Friedrichs, H. P. Hodson, and W. N. Dawes, "The Design of an Improved Endwall Film-Cooling Configuration," *J of Turbomachinery* 121 (1999): 772-780.
12. S. W. Burd, and T. W. Simon, "Effects of Slot Bleed Injection over a Contoured Endwall on Nozzle Guide Vane Cooling Performance: Part I: Flow Field Measurements," ASME Paper No. 2000-GT-199; S. W. Burd, C. J. Satterness, and T. W. Simon, "Effects of Slot Bleed Injection over a Contoured Endwall on Nozzle Guide Vane Cooling Performance: Part II Thermal Measurements," ASME Paper No. 2000-GT-200; R. Oke, T. Simon, S. W. Burd, and R. Vahlberg, "Measurements in a Turbine Cascade Over a Contoured Endwall: Discrete Hole Injection of Bleed Flow," ASME Paper Number 2000-GT-214; R. Oke, T. Simon, T. Shih, B. Zhu, Y.L. Lin, and M. Chyu, "Measurements Over a Film-Cooled, Contoured Endwall with Various Coolant Injection Rates," ASME Paper Number 2001-GT-140.
13. *Ibid.*
14. W. F. Colban, K. A. Thole, and G. Zess, "Combustor-Turbine Interface Studies: Part 1: Endwall Measurements," *J of Turbomachinery* 125 (2002): 193-202; W. F. Colban, A. T. Lethander, K. A. Thole, and G. Zess, "Combustor-Turbine Interface Studies: Part 2: Flow and Thermal Field Measurements," *J of Turbomachinery* 125 (2002): 203-209.
15. F. Kost and M. Nicklas, "Film-Cooled Turbine Endwall in a Transonic Flow Field: Part I – Aerodynamic Measurements," ASME Paper Number 2001-GT-0145 (2001); M. Nicklas, "Film-Cooled Turbine Endwall in a Transonic Flow Field: Part II – Heat Transfer and Film-Cooling Effectiveness Measurements," ASME Paper Number 2001-GT-0146 (2001).
16. D. K. Knost, and K. A. Thole, "Computational Predictions of Endwall Film-Cooling for a First Stage Vane," GT-2003-38252.
17. R. Bunker, "Turbine Blade Tip Design and Tip Clearance Treatment," von Karman Lecture Series 2004-02 (2003).
18. R. S. Bunker, "A Review of Turbine Blade Tip Heat Transfer," Turbine 2000 Symposium on Heat Transfer in Gas Turbine Systems, Cesme, Turkey, 2000.
19. Y. W. Kim and D. E. Metzger, "Heat Transfer and Effectiveness on Film Cooled Turbine Blade Tip Models," *J of Turbomachinery* 117 (1995); Y. W. Kim, J. P. Downs, F. O. Soechting, W. Abdel-Messeh, G. Steuber, and S. Tanrikut, "A Summary of the Cooled Turbine Blade Tip Heat Transfer and Film Effectiveness Investigations Performed by Dr. D. E. Metzger," *J of Turbomachinery* 117(1995): 1-11.
20. J. S. Kwak and J. C. Han, "Heat Transfer Coefficient and Film-Cooling Effectiveness on a Gas Turbine Blade Tip," GT2002-30194; J. S. Kwak and J. C. Han, "Heat Transfer Coefficient and Film-Cooling Effectiveness on the Squealer Tip of a Gas Turbine Blade," GT2002-30555.

4.2.3 Airfoil Endwall Heat Transfer

21. J. R. Christophel, K. A. Thole, and F. Cunha, "Cooling the Tip of a Turbine Blade Using Pressure Side Holes—Part 1: Film Effectiveness Measurements," *J of Turbomachinery* 127 (2005): 270-277; J. R. Christophel, K. Thole, and F. Cunha, "Cooling the Tip of a Turbine Blade Using Pressure Side Holes—Part 2: Heat Transfer Measurements," *J of Turbomachinery* 127 (2005): 278-286.



BIOGRAPHY

4.1 Introduction

4.2.3 Airfoil Endwall Heat Transfer



Karen Thole

William S. Cross Professor
Mechanical Eng. Dept, Penn State Univ.
University Park, PA 16802-1412

phone: (814) 865-2519
email: kthole@psu.edu

Dr. Karen Thole holds a Professorship in Mechanical Engineering at Penn State University. Her B.S. and M.S. degrees are in Mechanical Engineering from the University of Illinois, and her Ph.D. in Mechanical Engineering is from the University of Texas at Austin. After receiving her Ph.D. in 1992, she spent two years as a post-doctoral researcher at the University of Karlsruhe in Karlsruhe Germany. After her post-doctoral position, she accepted an assistant professor position at the University of Wisconsin-Madison where she taught and performed research in the Mechanical Engineering Department. In 1999 she accepted a position in the Mechanical Engineering Department at Virginia Tech where she was promoted to full professor in 2003. Dr. Thole's areas of expertise are heat transfer and fluid mechanics specializing in understanding high freestream turbulence effects. Over the past few years she has developed a number of unique testing facilities directed towards gas turbine heat transfer issues including a combustor simulator that simulates the flow field effects relevant to those entering the turbine section of an engine. Dr. Thole has been responsible for attracting research funding amounting to over \$4 million from such agencies at the Department of Energy, US Air Force, Pratt & Whitney, Modine Manufacturing, Siemens-Westinghouse and the National Science Foundation. She has published over 100 peer reviewed papers with a number of these presentations given to international audiences.